Evaluating density functional performance for the quasi-two-dimensional electron gas

2000 J. Phys.: Condens. Matter 12 1239

(http://iopscience.iop.org/0953-8984/12/7/308)

J. Phys.: Condens. Matter **12** (2000) 1239–1252. Printed in the UK PII: S0953-8984(00)09642-9

Evaluating density functional performance for the quasi-two-dimensional electron gas

L Pollack† and J P Perdew

Department of Physics and Quantum Theory Group, Tulane University, New Orleans, LA 70118, USA

Received 17 November 1999

Abstract. The exchange–correlation energy E_{xc} is a significant part of the total energy of the quasi-two-dimensional electron gas. We investigate the performance of three-dimensional density functionals $E_{xc}[n]$ in this system, showing how the local density approximation (LDA), the generalized gradient approximation (GGA), and the meta-GGA behave as functions of quantum well width or layer thickness. Shrinking the width in one direction is an example of non-uniform density scaling; we generalize the non-uniform scaling condition on the exact $E_{xc}[n]$ to densities $n(\boldsymbol{r})$ that are infinitely extended. We find that, although all three semi-local approximations break down as the true two-dimensional (zero-width) limit is approached (and as the reduced density gradients diverge almost everywhere), these approximations yield good results for wide quasi-two-dimensional systems. The simple liquid drop model provides unexpectedly accurate results for exchange–correlation energies of the quasi-two-dimensional electron gas, and an insight into the domain of validity of the standard functionals. An exact-exchange functional provides the correct approach to the true two-dimensional limit.

1. Introduction

In the past few decades, two-dimensional electronic systems have been realized in several experiments and devices. The electrons may be found trapped by image charges on the liquid ^{4}He surface [1], in the inversion layer of a metal–oxide–semiconductor system, or in a quantum well of a layered superlattice of two semiconductors such as AlGaAs/GaAs [2]. From a theoretical standpoint, these systems resemble the two-dimensional electron gas (2DEG) or two-dimensional jellium.

Since density functional theory [3–5] has proven useful for understanding both molecules and solids, it is natural to explore its role in electron systems of reduced dimensionality. Additionally, the two-dimensional gas is worthy of study for many reasons of its own. First, compared to three dimensions, the range of experimentally available electron densities is greater in two dimensions [6], which facilitates testing many-body predictions and observing new phenomena. Rajagopal and Kimball [7] and Dobson [8] have suggested that the 2DEG model may fit the experimental systems more closely than the 3DEG fits conduction electrons in metals. Second, electron correlations can be much stronger in 2D than in 3D, and quantum effects can become very pronounced [6, 9]. Lastly, the uniform electron gas is the basis of density functional theory and part of nature's data set (consider sodium, a metal whose bulk and surface properties are accurately given by the uniform electron gas model). Since this

† Current address: Department of Physics/Engineering, Xavier University, New Orleans, LA 70125, USA.

0953-8984/00/071239+14$30.00

simple system has forged understanding of many complicated problems in density functional theory, the 2DEG should be a logical starting point for studies in two dimensions.

The exchange–correlation energy of the 2D electron gas is our main concern here, although numerous properties of the 2DEG [10, 11] have been investigated in the last 30 years. Many-body effects such as exchange and correlation are especially important in systems like inversion layers on silicon or in certain quantum wells of GaAs, where the average distance between electrons in effective bohrs, r_s, is greater than unity, with the result that kinetic energy no longer dominates. Many-electron perturbation theory [7, 9, 12, 13] and quantum Monte Carlo methods [14–16] have been used to calculate the exchange–correlation energy. Ando [17, 18] was probably the first to calculate properties of the 2DEG with density functional theory. Using the local density approximation (LDA), and developing his own model of the electron gas for charge carriers in Si, Ando calculated charge density, effective masses, the g-factor, the self-consistent potential, and sub-band structure on Si(100) surface layers.

Using several functionals (the LDA, the generalized gradient approximation or GGA, and the meta-GGA), we calculate exchange–correlation energies for a 2DEG of finite thickness and examine how these functionals behave in the approach to the true 2D limit, as the thickness shrinks to zero [19]. One way to visualize our system is to consider the electrons confined between infinite potential barriers and to shrink the distance between barriers to zero. This infinite-barrier model lends itself to simple wavefunctions and has been used to study the jellium surface [20, 21]. We use it here, combined with the functionals mentioned above, to study the 2DEG of finite thickness. A strong confining potential, such as the infinite-barrier or the harmonic potential [22], is needed to approach the true 2D limit; self-consistent calculations for a jellium slab cannot approach this limit. Unlike the harmonic potential, our infinite barrier permits us to examine the liquid drop model for quasi-2D systems.

In the following sections, we set up our Kohn–Sham system of electrons subject to infinite barriers and then test three exchange–correlation functionals as they approach the true two-dimensional limit. This formulation of the problem is an application of non-uniform scaling [23, 24] of the density, which we discuss as well. The liquid drop model for metals will also be used as a simple yet surprisingly accurate way to find the exchange–correlation energy as a function of thickness. As we demonstrate, this process of shrinking the thickness to zero is a severe test for the local and semi-local functionals, which diverge in the exact two-dimensional limit. This failing was first noted by Kim *et al* [22], who used a harmonic quantum well model. Fully non-local functionals, such as the average density approximation [22] or the exact-exchange functional [25] considered here, may be needed for a proper approach to the true 2D limit.

By using the infinite-barrier model for the quantum well, we can make two investigations which we could not have made with the harmonic potential: testing the liquid drop model and the Seidl–Perdew–Levy [25] non-local density functional.

2. Infinite-barrier model for a quantum well

In our model quantum well, the Kohn–Sham potential v_s which confines the electrons is given by the infinite-barrier model [26] as

$$v_s(x, y, z) = \begin{cases} 0 & \text{if } 0 \leqslant x \leqslant L \\ \infty & \text{otherwise.} \end{cases} \tag{1}$$

This Kohn–Sham potential, acting on non-interacting electrons, produces $n(x)$, the density of the interacting electrons that we shall study. Using the potential v_s is expedient for two

reasons: it yields densities that are easy to work with and avoids the need to solve the Kohn–Sham equations self-consistently.

The 2D density parameter r_s^{2D} is the radius of the circle that encloses on average one electron and yields the density of electrons per unit area of the yz-plane:

$$n^{2D} = \frac{1}{\pi (r_s^{2D} a_0)^2} \tag{2}$$

where $a_0 = \hbar^2/me^2$ is the Bohr radius for jellium (or the effective Bohr radius $\hbar^2\epsilon/m^*e^2$ for a semiconductor with dielectric constant ϵ and effective mass m^*). Since we prefer atomic units where $\hbar = m = e^2 = 1$ (or $\hbar = m^* = e^2/\epsilon = 1$), all subsequent distances are given in bohrs (or effective bohrs) and all energies are given in hartrees $me^4/\hbar^2$ (or effective hartrees $m^*e^4/\hbar^2\epsilon^2$ for a semiconductor).

With the Kohn–Sham orbital

$$\psi_{\ell,k} = \frac{1}{\sqrt{AL}} \sqrt{2} \sin\left(\frac{\ell \pi x}{L}\right) e^{i(yk_y + zk_z)} \tag{3}$$

where A is a macroscopic area of the yz-plane, $\ell = 1, 2, 3, \ldots$ is the sub-band index, and k_i are the Bloch wavevector components for motion parallel to the surface, we solve the Schrödinger equation to find the energy levels

$$E_{\ell,k} = \frac{1}{2}\left[\left(\frac{\ell\pi}{L}\right)^2 + k_y^2 + k_z^2\right]. \tag{4}$$

When only the lowest level is occupied ($E_{1,k_F^{2D}} < E_{2,0}$), the density of states of this system begins to resemble the density of states of a 2D electron gas [2]. Here $k_F^{2D} = (2\pi n^{2D})^{1/2}$ is the two-dimensional Fermi wavevector, so

$$L < \sqrt{\frac{3}{2}}\pi r_s^{2D} = 3.85 r_s^{2D} = L_{max}. \tag{5}$$

When L falls in this range, motion along the x-direction is frozen out, the electrons only have two degrees of freedom along $\boldsymbol{y}$ and $\boldsymbol{z}$, and the system may be considered quasi-two-dimensional. $L \ll 3.85 r_s^{2D}$ yields the true two-dimensional limit, which can actually be realized in solid-state experiments with low areal densities n^{2D}. The 3D density of this quasi-two-dimensional system is then, from equation (3),

$$n(x) = \frac{2}{L\pi (r_s^{2D})^2} \sin^2\left(\frac{\pi x}{L}\right) \tag{6}$$

for $0 \leqslant x \leqslant L$, and zero otherwise. (Note that the 2D Fermi wavelength is $2\pi/(\sqrt{2}/r_s^{2D}) = 4.44 r_s^{2D}$.)

3. Functionals and non-uniform density scaling

The ground-state energy of the homogeneous electron gas is

$$E = T_s + E_x + E_c. \tag{7}$$

For any density $n(\boldsymbol{r})$, E_x and E_c are defined in references [3,4]. (For a discussion of the density fluctuations that contribute to E_x and E_c in one, two, or three dimensions, and for a related definition of 'correlation strength', see reference [27].) The non-interacting kinetic energy, T_s, can be found exactly from the Kohn–Sham orbitals, but the exchange and correlation energy density functionals, E_x and E_c respectively, are usually approximated. In this paper we test the

following exchange and correlation functionals: the local density approximation [28] (LDA), the generalized gradient approximation [29–32] (GGA), and the meta-GGA [33,34] (MGGA).

For calculations involving the solid state, the LDA has been very successful [3,4], working best for cases of slowly varying density. For our model quantum well of thickness L, we evaluate the LDA exchange–correlation energy per particle

$$\frac{E_{xc}^{LDA}}{N} = \left(\int_0^L n(x)\varepsilon_{xc}^{unif}(n(x))\,\mathrm{d}x\right)\Big/\int_0^L n(x)\,\mathrm{d}x \tag{8}$$

where ε_{xc}^{unif} is the exchange–correlation energy per particle of the three-dimensional uniform electron gas [28] and $\varepsilon_{xc} = \varepsilon_x + \varepsilon_c$. We use an ε_c^{unif} parametrized in reference [35], while the exchange energy per particle for the uniform electron gas is the well known

$$\varepsilon_x^{unif} = -\frac{3}{4\pi}(3\pi^2 n)^{1/3} = -\frac{3}{4\pi}\frac{(9\pi/4)^{1/3}}{r_s^{3\mathrm{D}}}. \tag{9}$$

Here $r_s^{3\mathrm{D}}$ is the familiar local density parameter that measures the radius of the sphere enclosing one electron in a 3D system. In the LDA, and in the subsequent GGA and MGGA calculations, the r_s-input required for the functionals is the parameter $r_s^{3\mathrm{D}}$. For calculations with the functionals, we used an $r_s^{3\mathrm{D}}$ defined as

$$n^{3\mathrm{D}} = \frac{3}{4\pi(r_s^{3\mathrm{D}})^3} \tag{10}$$

with $n^{3\mathrm{D}}$ given by $n(x)$ in equation (6).

Perdew, Burke, and Ernzerhof (PBE) [32] developed a simplified GGA for exchange and correlation, which we will test for our model quantum well:

$$\frac{E_{xc}^{GGA}}{N} = \left(\int_0^L n(x)\varepsilon_{xc}^{GGA}(n(x), \nabla n(x))\,\mathrm{d}x\right)\Big/\int_0^L n(x)\,\mathrm{d}x. \tag{11}$$

An alternative derivation of the PBE GGA is given in reference [36]. Like the LDA, the PBE GGA is non-empirical.

The meta-GGA incorporates additional semi-local information into the functional, namely the kinetic energy density τ of the occupied Kohn–Sham orbitals. We use the meta-GGA of Perdew, Kurth, Zupan, and Blaha [33, 34] to study

$$\frac{E_{xc}^{MGGA}}{N} = \left(\int_0^L n(x)\varepsilon_{xc}^{MGGA}(n(x), \nabla n(x), \tau(x))\,\mathrm{d}x\right)\Big/\int_0^L n(x)\,\mathrm{d}x. \tag{12}$$

Before making any numerical studies, we can obtain useful insights into the functionals from scaling arguments. A helpful tool in a density functional analysis is coordinate scaling, because it presents a set of criteria [37] that exact functionals should meet; these conditions can serve as a guide when developing and testing approximate functionals. A uniformly scaled density is

$$n_\lambda(x, y, z) = \lambda^3 n(\lambda x, \lambda y, \lambda z) \tag{13}$$

in which λ, the parameter that controls scaling, acts on all three coordinates. The exact condition $E_x[n_\lambda] = \lambda E_x[n]$ [38] is satisfied by all popular approximate functionals. The process of scaling allows one to contract or expand the density but still maintain normalization; i.e.,

$$\int n\,\mathrm{d}^3r = \int n_\lambda\,\mathrm{d}^3r = N.$$

In our system, only a single coordinate will shrink. This is an example of non-uniform scaling [23, 39] in one dimension, namely

$$n_\lambda^x(x, y, z) = \lambda n(\lambda x, y, z). \tag{14}$$

Clearly the scaling only affects the x-coordinate, and the high-density limit is reached as $\lambda \to \infty$. From equation (6) we can find our scaled density

$$n_\lambda^x(x) = \frac{2}{(L/\lambda)\pi(r_s^{2D})^2} \sin^2\left(\frac{\pi x}{L/\lambda}\right). \tag{15}$$

The parameter (L/λ) controls the scaling such that the true two-dimensional limit ($L/\lambda \ll 3.85 r_s^{2D}$) is achieved when $\lambda \to \infty$. To illustrate the effect of increasing λ (where $\lambda = 1$ recovers the original density), figure 1 shows the result of scaling by a factor of two and five respectively. As well width L decreases to $L/2$ and then to $L/5$, the density in the x-direction grows more compact.

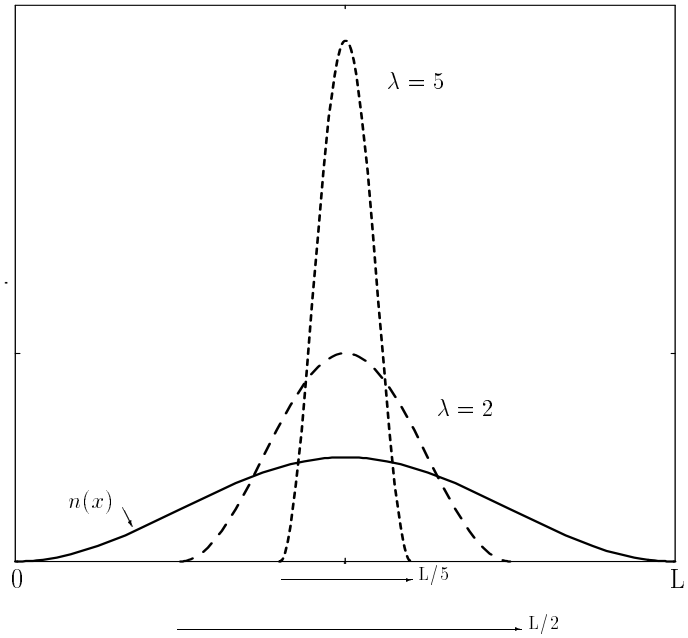

Figure 1. An example of coordinate scaling of a quantum well density. The original density $n(x)$ is related to the scaled density such that $n_\lambda(x) = \lambda n(\lambda x)$. Note how the high-density limit starts to take shape as λ is increased to 2 then 5. The original density is $n(x) = n_{\lambda=1}(x)$.

The behaviour of the exact-exchange and correlation functionals that results from non-uniform scaling in the high-density limit is [24]

$$\lim_{\lambda\to\infty} E_x[n_\lambda^x] > -\infty \tag{16}$$

and

$$\lim_{\lambda\to\infty} E_c[n_\lambda^x] = 0. \tag{17}$$

The LDA, PBE GGA, and MGGA violate [40, 41] the condition of equation (16). Only the PBE GGA and MGGA meet the correlation scaling requirement of equation (17). Since all three functionals mentioned above fail to meet the non-uniform scaling requirements of

equation (16), we can predict that they will not yield finite exchange–correlation energies for the exact 2DEG of zero thickness. In the same way, these functionals fail for strong non-uniform scaling of a hydrogen atom [41] or a quantum dot [22]. However, they work well [22] for quantum dots in experimentally realistic configurations.

It appears to us that the derivations of equations (16) and (17) do not apply to the density of equation (15), which is infinitely extended in the y- and z-directions. Since the exchange and correlation energies per electron are known [11] to tend to finite negative constants in the exact 2D limit ($L \to 0$), the generalized non-uniform scaling relations are probably

$$\lim_{\lambda\to\infty} \frac{1}{N} E_x[n_\lambda^x] > -\infty \tag{18}$$

and

$$\lim_{\lambda\to\infty} \frac{1}{N} E_c[n_\lambda^x] > -\infty \tag{19}$$

for a density $n(\boldsymbol{r})$ that is finite along the x-direction. For the 3D uniform gas, which is not finite along any direction, the exchange energy per electron diverges to minus infinity like $\lambda^{1/3}$, and the correlation energy per electron like $\ln\lambda$, as $\lambda \to \infty$ under one-dimensional scaling.

Even for a finite system, we suspect that the '=0' on the right of equation (17) should be replaced by '$>-\infty$', since an infinite system is only the limit of a sequence of finite ones, and the limit of a sequence of zeros can only be zero.

4. Numerical tests of the functionals

Even though, from scaling arguments mentioned above, we expect the approximate exchange functionals to break down as zero thickness is approached, the quasi-two-dimensional regime of finite thickness is also of interest. In fact exchange as a function of layer thickness has been calculated [42,43] exactly using the orbitals of equation (3); see equation (13) of reference [43]. Therefore in figure 2, we compare approximate exchange functionals to the exact result as a function of layer thickness.

We note that the GGA and MGGA graphs look identical and for clarity of viewing we only show the GGA results. As can be seen in figure 2, the LDA and the GGA are accurate until the quantum well width L grows smaller than the average planar distance between electrons. In the region where $L \gg r_s^{2D}$, the GGA does a slightly better job than the LDA in matching the exact result. However, all three functionals that we tested seem to do well in this region.

In two dimensions, there have been numerous studies of the exchange–correlation energy [7, 9, 15, 16, 44]. One expression [25] that interpolates realistically between the high- and low-density (Wigner crystal) limits is

$$\varepsilon_x^{2D} = \frac{-0.6002}{r_s^{2D}} \qquad \varepsilon_c^{2D} = 0.5058\left[\frac{1.3311}{(r_s^{2D})^2}\left(\sqrt{1+1.5026\,r_s^{2D}}-1\right)-\frac{1}{r_s^{2D}}\right]. \tag{20}$$

We use equation (20) to determine the true two-dimensional energies.

The behaviours of the correlation functionals are shown in figure 3. As expected from scaling arguments, the GGA curve approaches zero but the LDA approaches a negative, logarithmically infinite value. According to figure 3, an interesting contradiction arises. We see that, as $L \to 0$, the PBE GGA curve tends toward zero, following the non-uniform scaling prediction of equation (17); it does not approach the exact 2D correlation energy as given in equation (20). A possible resolution of this discrepancy was discussed at the end of the preceding section.

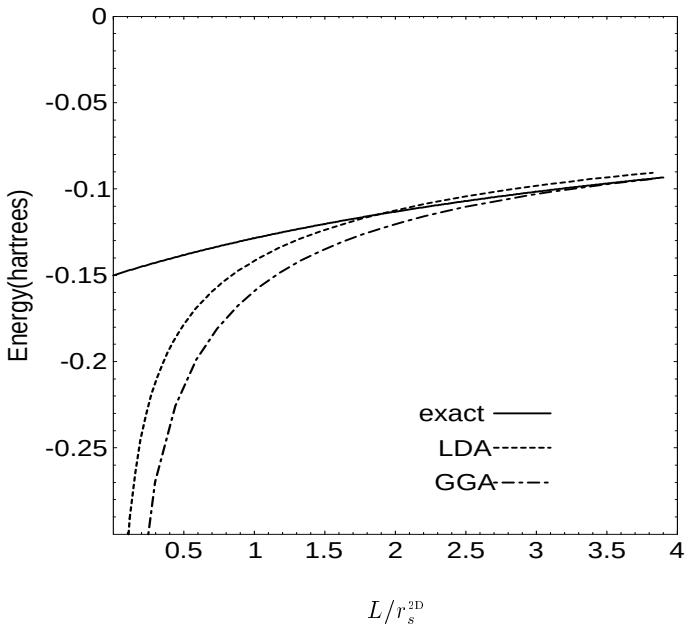

Figure 2. The exchange energy per electron as a function of thickness, for our model quantum well with $r_s^{2D} = 4$. The solid line is the exact-exchange energy as a function of thickness (see equation (13) of reference [43]). The PBE GGA and LDA are shown alongside this curve.

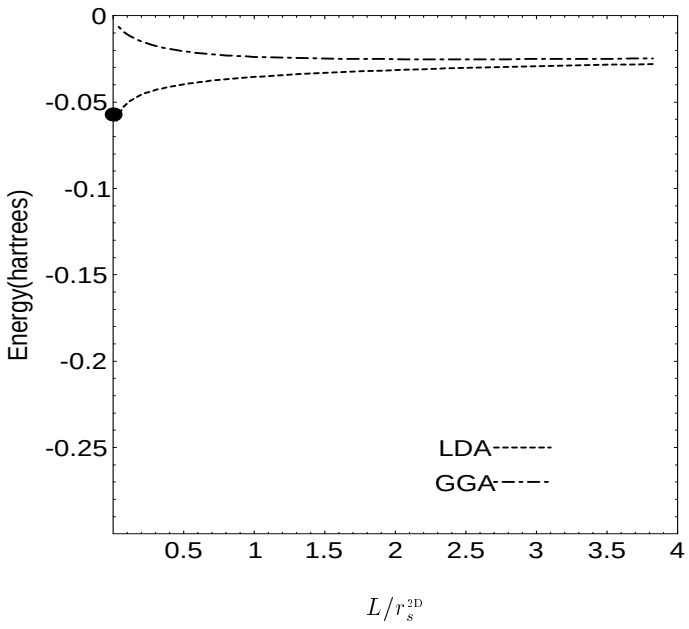

Figure 3. The correlation energy per electron as a function of thickness for our model quantum well. The LDA and PBE GGA functionals are shown for $r_s^{2D} = 4$. The exact value of the true 2D correlation energy, as calculated from equation (20) in the text, is represented as the dot on the vertical axis. The PBE correlation energy approaches zero in the limit of vanishing thickness, while the LDA correlation diverges logarithmically to minus infinity.

We can look at the $L \to 0$ behaviour of the PBE GGA exchange and correlation energies from another perspective, by examining the reduced density gradient

$$s = \frac{3}{2(9\pi/4)^{1/3}} |\nabla r_s^{3D}|. \tag{21}$$

In a 3D system, s, a key ingredient in the GGA, reveals how fast the density is varying on the scale of the local Fermi wavelength $\lambda_F^{3D} = 2\pi r_s^{3D}/(9\pi/4)^{1/3}$. Values of $s > 1$ indicate densities that are varying rapidly. In figure 4 we show this density gradient and its rapid increase as L shrinks. The divergence of s almost everywhere as $L \to 0$ shows that the density variation in this limit becomes too rapid for either LDA or GGA to work accurately.

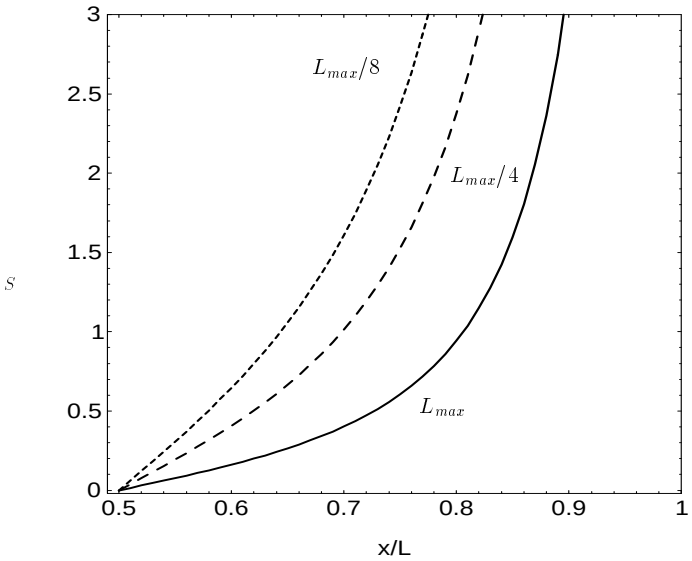

Figure 4. How the reduced density gradient $s(x)$ depends on well width L. Here $s = |\nabla n|/2k_F n$ (where $k_F = (3\pi^2 n)^{1/3}$) measures how fast the density varies on the scale of the local 3D Fermi wavelength. The solid curve represents $L = L_{max}$, and the next two dashed curves represent $L = L_{max}/4$ and $L_{max}/8$ respectively, where L_{max} is given by equation (5). For any given value of x/L, s increases as L shrinks, indicating a more rapid variation in the density. In general, $s > 1$ is associated with rapidly varying densities.

In a 3D system, λ_F^{3D} is also approximately the range of the exchange hole around an electron. The LDA exchange hole is a sphere of radius $\sim r_s^{3D} \sim \lambda_F^{3D}$. For a quasi-2D system, $r_s^{3D} \sim L^{1/3}$ at fixed r_s^{2D}; as $L \to 0$, the LDA exchange energy per electron of equation (9) diverges to minus infinity like $L^{-1/3}$ (figure 2). However, the *exact* exchange hole is a 'pancake' of thickness L and radius r_s^{2D}; as $L \to 0$, the exact-exchange energy per electron approaches a negative constant $\sim 1/r_s^{2D}$.

We expect LDA or GGA to work better for the combined exchange–correlation energy than for either exchange or correlation alone. A plot of these energies together is shown in the next section.

5. Liquid drop model and surface energies

Simple models are often useful for understanding complicated systems. One of the simplest ways to evaluate the energy of the quasi-two-dimensional electron gas is to use the liquid drop

model (LDM) for crystalline metals [45, 46]. In this model, the total energy of an extended system is given by contributions from bulk and surface terms (and a curvature term which we may ignore):

$$E^{LDM} = \alpha V + \sigma \int \mathrm{d}A + \cdots \tag{22}$$

where V is the volume and $\mathrm{d}A$ is an element of surface area. Here α and σ are the volume and surface energies of the 3D uniform electron gas. Our model quantum well has a bulk region and two planar surfaces, each of area A.

Because the liquid drop model defines a system with a bulk thickness $L_b < L$, where L_b is the thickness of the positive background of density $3/(4\pi(r_{s,b}^{3\mathrm{D}})^3)$, we need an expression for the 3D bulk or background density parameter $r_{s,b}^{3\mathrm{D}}$. By minimizing the electrostatic moments in the appendix, we derive

$$L_b = \sqrt{1 - \frac{6}{\pi^2}}\,L \tag{23}$$

$$r_{s,b}^{3\mathrm{D}} = \left(\frac{3}{4}\right)^{1/3}\left(1 - \frac{6}{\pi^2}\right)^{1/6}\left(L(r_s^{2\mathrm{D}})^2\right)^{1/3}. \tag{24}$$

Now for $V = AL_b$, we calculate an exchange–correlation energy per particle for our quasi-2D system as a function of the bulk density parameter $r_{s,b}^{3\mathrm{D}}$:

$$\varepsilon_{xc}^{LDM} = \frac{E_{xc}^{LDM}}{N} = \frac{\alpha_{xc}V}{N} + 2\frac{\sigma_{xc}A}{N} = \varepsilon_{xc}^{unif}(r_{s,b}^{3\mathrm{D}}) + 2\pi(r_s^{2\mathrm{D}})^2\sigma_{xc}(r_{s,b}^{3\mathrm{D}}) \tag{25}$$

where ε_x^{unif} is given by equation (9), and ε_c^{unif} is found in reference [35].

We tried three different surface exchange–correlation energies for the infinite-barrier model in equation (25): σ_{xc}^{LDA}, σ_{xc}^{PBE}, σ_{xc}^{exact}. The 'exact' value is from a short-range correlation correction [47] to the random-phase approximation [48]. Because $r_{s,b}^{3\mathrm{D}}$ decreases as L shrinks for a given $r_s^{2\mathrm{D}}$, we found $\sigma_{xc}(r_{s,b}^{3\mathrm{D}})$ from a fit of calculated values for $r_{s,b}^{3\mathrm{D}} = 0$, 2.07, 4.0, and 6.0 to the interpolation formula

$$\sigma_{xc} \approx \frac{A}{(r_{s,b}^{3\mathrm{D}})^3}\frac{1 + Br_{s,b}^{3\mathrm{D}}}{1 + Cr_{s,b}^{3\mathrm{D}}}. \tag{26}$$

The parameters are $A^{exact} = 0.004\,068$, $B^{exact} = 3.451$, $C^{exact} = 1.688$, $A^{LDA} = 0.006\,318$, $B^{LDA} = 0.1885$, $C^{LDA} = 0.1245$, and $A^{PBE} = 0.002\,575$, $B^{PBE} = 2.131$, $C^{PBE} = 0.6762$. According to Newns [26], the infinite-barrier model is closest to self-consistent semi-infinite-jellium calculations [49] at $r_{s,b}^{3\mathrm{D}} = 5$.

In figure 5, we show ε_{xc}^{LDM} as a function of thickness, using σ_{xc}^{exact}. We also show the total exchange–correlation energy per particle given by the PBE GGA and LDA functionals. The simple liquid drop model works surprisingly well for very thin electron gas layers. Although it also fails as $L \to 0$, it provides a better approach to the true 2D limit than either the LDA or PBE GGA functional. In all our figures, we show energies for $r_s^{2\mathrm{D}} = 4$, for which the infinite-barrier model can be fairly realistic.

The liquid drop model can also provide an intuitive, simple-metal example of a quasi-2D system. Consider a monolayer of sodium atoms lying in the close-packed 110 plane with bulk spacing. For this system, $r_{s,b}^{3\mathrm{D}} = 3.93$, $L_b = 1.436r_{s,b}^{3\mathrm{D}} = 5.64$ [50], and $L = 9.01$. Thus $r_s^{2\mathrm{D}} = 3.79$ and $L/r_s^{2\mathrm{D}} = 2.38$. This is roughly the smallest ratio $L/r_s^{2\mathrm{D}}$ for which the LDA and GGA functionals work, and in fact LDA has been applied to a system rather like this one [51]. The functionals work well for a single normal atom or for a system built up from

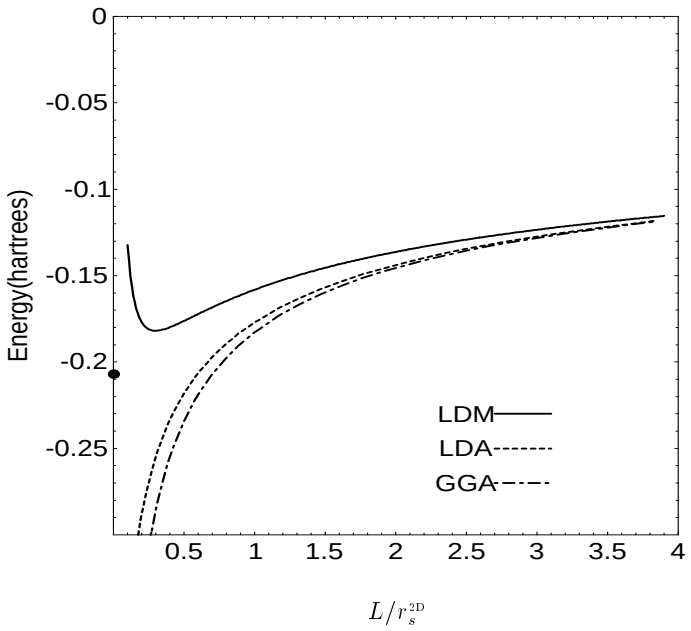

Figure 5. The liquid drop model (LDM) of equation (25) for our model quantum well at $r_s^{2D} = 4$, using an exact surface exchange–correlation energy σ_{xc}^{exact}. (The surface energy term of equation (25) contributes -6% at $L/r_s^{2D} = 3.85$, and -16% at $L/r_s^{2D} = 1$.) The PBE GGA and LDA functionals are shown alongside this curve. The exact-exchange–correlation energy per electron for $L \to 0$ is represented as a dot on the vertical axis.

such atoms. Values of L/r_s^{2D} less than 2.38 correspond to a non-spherical distortion of the atoms under uni-axial compression, for which the LDA and GGA are known to fail [22, 41].

Although the liquid drop model works very well for small well widths, most real-world devices cannot achieve zero thickness of a quantum well. Is it useful even to consider this $L \to 0$ limit? To answer this question, we look to the quantum wells of semiconductor interface devices. For a GaAs quantum well of width $L = 70$ Å and hole density $n^{2D} = 3.0 \times 10^{11}$ heavy holes cm^{-2}, which was used in far-infrared absorption spectroscopy [52] of the intersubband energy spacing in GaAs/(Al, Ga)As, we find $\epsilon = 12.9$, $m^*/m = 0.45$ [53], the effective bohr $= 15.2$ Å, $r_s^{2D} = 6.8$, and $L/r_s^{2D} = 0.68$. Because this system is close to the true 2D limit, that limit is in fact of physical interest. While a two-dimensional LDA can be made (using equation (20) of this paper or equation (14) of reference [15] for example), there is still a need for a density functional that can span the whole range of quantum well widths. Merely satisfying equation (18), as in the GGA of reference [54], is not sufficient [22], since equation (18) provides little guidance as regards the value of the limiting constant for the left-hand side of equation (18).

6. Failure of the meta-GGA, and the correct approach to the true 2D limit

LDA and GGA are semi-local approximations which construct an energy density at position $\boldsymbol{r}$ from information available at $\boldsymbol{r}$ (such as $n(\boldsymbol{r})$) or from an infinitesimal neighbourhood (such as $\nabla n(\boldsymbol{r})$). Meta-GGAs make use of additional semi-local information, such as the Kohn–Sham orbital kinetic energy density $\tau(\boldsymbol{r})$. The meta-GGA of references [33, 34] is a controlled extrapolation from all known gradient expansions for slowly varying densities. In

comparison with GGA, it seems to give a better overall description of both atomization energies for molecules and equilibrium properties of solids and surfaces [34]. However, for the energy of the narrow quasi-2D quantum well, it fails (see figure 6) in about the same way as GGA.

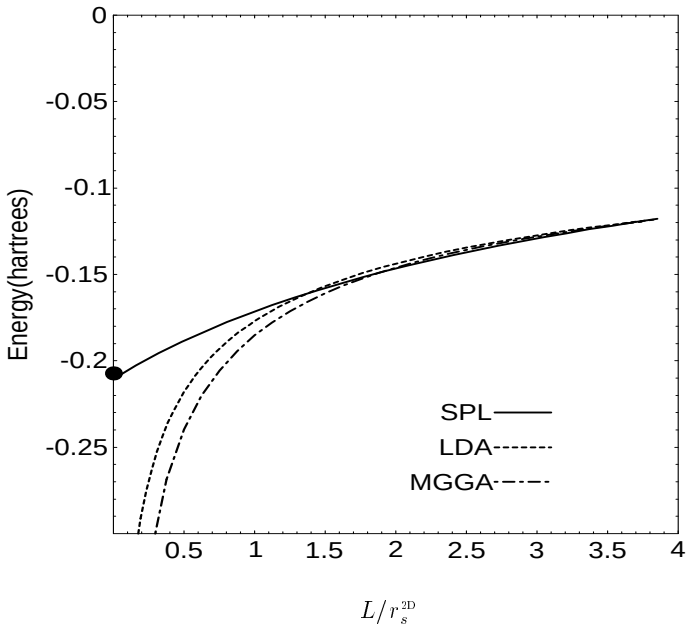

Figure 6. Seidl–Perdew–Levy (SPL) exchange–correlation energy per electron as a function of thickness, for our model quantum well with $r_s^{2D} = 4$. The LDA and meta-GGA functionals are shown alongside this curve. The exact-exchange–correlation energy per electron for $L \to 0$ is represented as a dot on the vertical axis.

Thus the approach to the true 2D limit seems to require a fully non-local density functional, in which the exchange–correlation energy density at position $\boldsymbol{r}$ is determined by information from all positions $\boldsymbol{r}'$.

A fully non-local approach, which makes use of the exact-exchange energy and is correct in the true 2D limit, has been suggested by Seidl, Perdew, and Levy [25]. They begin with the adiabatic connection formula

$$E_{xc}[n] = \int_0^1 \mathrm{d}\alpha \; W_\alpha[n] \tag{27}$$

where $W_\alpha[n]$ is the potential energy of exchange and correlation for a system of electrons with fixed density $n(\boldsymbol{r})$ and variable electron–electron interaction $\alpha/|\boldsymbol{r}' - \boldsymbol{r}|$. Equation (7) of reference [25] models the α-dependence of the integrand of equation (27), using only the exact-exchange energy $E_x = W_0$, the second-order Görling–Levy correlation energy $E_c^{GL2} = \frac{1}{2}\,\mathrm{d}W_\alpha/\mathrm{d}\alpha|_{\alpha=0}$, and the strong-interaction limit W_∞.

Two of the three ingredients needed for the quasi-2D quantum well in the infinite-barrier model are available from reference [43]: E_x from equation (13), and E_c^{GL2} from equation (45). For W_∞, we cannot use the three-dimensional 'PC model' of reference [25], which works well for atoms and molecules [55] but fails for the more rapid density variations of the infinite-barrier model. Instead we use the interpolation formula for $r_s^{2D} = 4$

$$W_\infty(L) = \left[1.918\left(1 - \frac{L}{L_{max}}\right) + 1.556\left(\frac{L}{L_{max}}\right)\right] W_0(L) \tag{28}$$

where $W_\infty(L = 0) = (8/3\pi - 2)/r_s^{2D}$ is given by the two-dimensional PC model [25], and $W_\infty(L = L_{max})$ is adjusted to reproduce the meta-GGA value for E_{xc} at $L = L_{max}$ ($W_\infty(L = L_{max}) = -0.146$ hartrees per electron for $r_s^{2D} = 4$).

With these inputs, equation (8) of reference [25] yields the curve in figure 6 which shows a correct approach to the true 2D limit. Note that second-order perturbation theory by itself is very inadequate at $r_s^{2D} = 4$ and $L \leqslant L_{max}$, where $E_c^{GL2} \approx 3E_c$.

7. Conclusions

Semi-local density functionals (LDA, GGA, meta-GGA) work for atoms, molecules, bulk solids, and solid surfaces [34]. They also work for atomic monolayers and other wide quasi-2D systems, but they fail as the true 2D limit is approached. The liquid drop model also fails in this zero-thickness limit, although surprisingly it seems to work over a greater range of finite thicknesses for quasi-2D systems. Fully non-local functionals (e.g., those that incorporate exact-exchange) may be needed to describe the approach to the true 2D limit.

Semi-local approximations can only be expected to work when typical [56] dimensionless density gradients (e.g., equation (21)) are not too large. In the approach to the true 2D limit, as in the one-dimensional scaling of equations (16) and (17), these dimensionless gradients diverge almost everywhere. As discussed elsewhere [57], there is no universal large-gradient behaviour that can be expressed in semi-local form. The problem remains to construct a simple, practical density functional for E_{xc} which behaves properly under non-uniform density scaling.

Acknowledgments

We thank Richard M Martin, Yong-Hoon Kim, and Christoph Grein for discussions. This work was supported by the US National Science Foundation under Grant No DMR98-10620. One of us (LP) was supported in part by the Louisiana Educational Quality Support Fund.

Appendix A. Bulk or background density

We derive an expression for the bulk density parameter $r_{s,b}^{3D}$ as a function of L and r_s^{2D}. In the infinite-barrier model for the quasi-2D electron gas in a quantum well of width L, the positive background charge density $n_+(x)$ is a step function:

$$n_+(x) = \begin{cases} n_b & -L_b/2 \leqslant x \leqslant L_b/2 \\ 0 & \text{otherwise} \end{cases} \tag{A.1}$$

which does not come right up to the surface of the quantum well. This surface, shown in figure A1, is at $(-L/2, L/2)$. The electron density, however, fully extends to the potential barrier and is given by

$$n_-(x) = \frac{2}{\pi L (r_s^{2D})^2} \cos^2\left(\frac{\pi x}{L}\right). \tag{A.2}$$

The charge density is $n_+(x) - n_-(x)$. For convenience, we have relocated the origin to the centre of the well.

The best way to determine the parameters L_b and n_b is to impose both the conditions of electrical neutrality and minimization of the electrostatic energy. However, a simpler

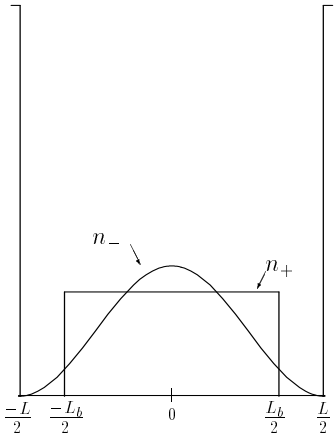

Figure A1. The quasi-two-dimensional electron gas in an infinite-barrier potential of width L. The electron density profile n_- is shown. The positive background n_+ is represented as a step function that does not extend to the surfaces of the barriers.

alternative that is almost equivalent is to match the first three multipole moments of $n_-(x)$ and $n_+(x)$ about the mid-point $x = 0$:

$$\int_{-\infty}^{\infty} \mathrm{d}x\; n_-(x) = \int_{-\infty}^{\infty} \mathrm{d}x\; n_+(x) \tag{A.3}$$

$$\int_{-\infty}^{\infty} \mathrm{d}x\; xn_-(x) = \int_{-\infty}^{\infty} \mathrm{d}x\; xn_+(x) \tag{A.4}$$

$$\int_{-\infty}^{\infty} \mathrm{d}x\; x^2 n_-(x) = \int_{-\infty}^{\infty} \mathrm{d}x\; x^2 n_+(x). \tag{A.5}$$

This yields equation (23). The bulk density can be written as

$$n_b = \frac{1}{L_b \pi (r_s^{2\mathrm{D}})^2} = \frac{3}{4\pi (r_{s,b}^{3\mathrm{D}})^3}. \tag{A.6}$$

We can solve (A.6) for $r_{s,b}^{3\mathrm{D}}$ to find equation (24).

References

[1] Cole M W 1974 *Rev. Mod. Phys.* **46** 451
[2] Weisbuch C and Vinter B 1991 *Quantum Semiconductor Structures* (Boston, MA: Academic)
[3] Jones R O and Gunnarsson O 1989 *Rev. Mod. Phys.* **61** 689
[4] Parr R G and Yang W 1989 *Density Functional Theory of Atoms and Molecules* (New York: Oxford University Press)
[5] Kohn W, Becke A D and Parr R G 1996 *J. Phys. Chem.* **100** 12 974
[6] Isihara A 1989 *Solid State Physics* vol 42, ed H Ehrenreich and D Turnbull (Boston, MA: Academic) p 271
[7] Rajagopal A K and Kimball J C 1977 *Phys. Rev.* B **15** 2819
[8] Dobson J F 1995 *Density Functional Theory (NATO ASI Series)* ed E K U Gross and R M Dreizler (New York: Plenum)
[9] Isihara A and Ioriatti L 1980 *Phys. Rev.* B **22** 214
[10] Ando T, Fowler A B and Stern F 1982 *Rev. Mod. Phys.* **54** 437
[11] Rajagopal A K 1998 *Strongly Coupled Coulomb Systems* ed G J Kalman, J M Rommel and K Blagoev (New York: Plenum) p 49
[12] Stern F 1973 *Phys. Rev. Lett.* **30** 278

[13] Kalia R K, Kawamoto G, Quinn J J and Ying S C 1980 *Solid State Commun.* **34** 423
[14] Ceperley D 1978 *Phys. Rev.* B **18** 3126
[15] Tanatar B and Ceperley D M 1989 *Phys. Rev.* B **39** 5005
[16] Kwon Y, Ceperley D M and Martin R M 1993 *Phys. Rev.* B **48** 12 037
[17] Ando T 1976 *Phys. Rev.* B **13** 3468
[18] Ando T 1976 *Surf. Sci.* **58** 128
[19] Pollack L 1999 *PhD Thesis* Tulane University
[20] Harris J and Jones R O 1974 *J. Phys. F: Met. Phys.* **4** 1170
[21] Mahan G D 1975 *Phys. Rev.* B **12** 5585
[22] Kim Y-H, Lee I-H, Nagaraja S, Leburton J-P, Hood R Q and Martin R M 2000 *Phys. Rev.* B **61**
[23] Levy M and Ou-Yang H 1990 *Phys. Rev.* A **42** 651
[24] Görling A and Levy M 1992 *Phys. Rev.* A **45** 1509
[25] Seidl M, Perdew J P and Levy M 1999 *Phys. Rev.* A **59** 51
[26] Newns D M 1970 *Phys. Rev.* B **1** 3304
[27] Ziesche P, Tao J, Seidl M and Perdew J P 2000 *Int. J. Quantum Chem.* at press
[28] Kohn W and Sham L J 1965 *Phys. Rev.* **140** A1133
[29] Langreth D C and Mehl M J 1983 *Phys. Rev.* B **28** 1809
[30] Becke A D 1988 *Phys. Rev.* A **38** 3098
[31] Perdew J P and Wang Y 1986 *Phys. Rev.* B **33** 8800
Perdew J P and Wang Y 1989 *Phys. Rev.* B **40** 3399 (erratum)
[32] Perdew J P, Burke K and Ernzerhof M 1996 *Phys. Rev. Lett.* **77** 3865
Perdew J P, Burke K and Ernzerhof M 1997 *Phys. Rev. Lett.* **78**, 1396 (erratum)
[33] Perdew J P, Kurth S, Zupan A and Blaha P 1999 *Phys. Rev. Lett.* **82** 2544
Perdew J P, Kurth S, Zupan A and Blaha P 1999 *Phys. Rev. Lett.* **82** 5179 (erratum)
[34] Kurth S, Perdew J P and Blaha P 1999 *Int. J. Quantum Chem.* **75** 889
[35] Perdew J P and Wang Y 1992 *Phys. Rev.* B **45** 13 244
[36] Perdew J P, Burke K and Wang Y 1996 *Phys. Rev.* B **54** 16 533
[37] Levy M and Perdew J P 1994 *Int. J. Quantum Chem.* **49** 539
[38] Levy M and Perdew J P 1985 *Phys. Rev.* B **32** 2010
[39] Ou-Yang H and Levy M 1990 *Phys. Rev.* A **42** 155
[40] Levy M and Perdew J P 1993 *Phys. Rev.* B **48** 11 683
[41] Kurth S 2000 *J. Mol. Struct. (Theochem)* at press
[42] Totsuji H, Tachibana H, Totsuji C and Nara S 1995 *Phys. Rev.* B **51** 11 148
[43] Betbeder-Matibet O, Combescot M and Tanguy C 1996 *Phys. Rev.* B **53** 12 929
[44] Vinter B 1975 *Phys. Rev. Lett.* **35** 1044
[45] Perdew J P, Wang Y and Engel E 1991 *Phys. Rev. Lett.* **66** 508
[46] Perdew J P, Ziesche P and Fiolhais C 1993 *Phys. Rev.* B **47** 16 460
[47] Yan Z, Kurth S and Perdew J P 1999 *Phys. Rev.* B submitted
[48] Pitarke J M and Equiluz A G 1999 private communication
[49] Lang N and Kohn W 1970 *Phys. Rev.* B **1** 4555
[50] Monnier R and Perdew J P 1978 *Phys. Rev.* B **17** 2595
[51] Reimann S M, Koskinen M, Häkkinen H, Lindelof P E and Manninen M 1997 *Phys. Rev.* B **56** 12 147
[52] Cole B E, Chamberlain J M, Henini M, Nakov V and Gobsch G 1996 *J. Appl. Phys.* **80** 6058
[53] Singh J 1993 *Physics of Semiconductors and their Heterostructures* (New York: McGraw-Hill)
[54] Perdew J P, Chevary J A, Vosko S H, Jackson K A, Pederson M R, Singh D J and Fiolhais C 1992 *Phys. Rev.* B **46** 6671
Perdew J P, Chevary J A, Vosko S H, Jackson K A, Pederson M R, Singh D J and Fiolhais C 1993 *Phys. Rev.* B **48** 4978 (erratum)
[55] Seidl M, Perdew J P and Kurth S 1999 *Phys. Rev. Lett.* submitted
[56] Zupan A, Burke K, Ernzerhof M and Perdew J P 1998 *J. Chem. Phys.* **108** 1522
[57] Burke K, Perdew J P and Wang Y 1998 *Electronic Density Functional Theory: Recent Progress and New Directions* ed J F Dobson, G Vignale and M Das (New York: Plenum)